ISSN 1027-5495. Functional Materials, 27, No.1 (2020), p. 170-178.
doi:https://doi.org/10.15407/fm27.01 .170

Analysis of anisotropy of the Young's modulus of ideal orientation of α-iron textures

N.A.Volchok, D.A.Dyachok, Z.A.Briukhanova, E.V.Dyshlov

South Ukrainian National Pedagogical University named K.Ushinsky, 26 Staroportofrankovska Str., 65020 Odesa, Ukraine

Received May 21, 2019

Using the Fourier analysis method, we studied the anisotropy of the Young's modulus (*E*) in the crystallographic planes of the main ideal orientations (IO) of the textures in α-iron sheets. The dependences of *E* on the direction of measurement, the anisotropy coefficients and the average values of *E* for the various IOs of annealing and rolling textures in α-iron are obtained. The texture of low-carbon DC04 (0.06 % C, up to 0.35 % Mn, up to 0.40 % Si, ~ 0.025 % S and P) steel sheets after annealing and cold rolling was investigated. The IO set of annealed sheets provides anisotropy of *E* with a maximum in the transverse direction (TD) and a minimum in the rolling direction (RD) + 45°. The process of rolling forms IOs which increase the Young's modulus in the TD and RD + 45°. The experimental values of *E* are in satisfactory agreement with the results of the calculations from the anisotropy of the IO obtained from an X-ray texture experiment.

Keywords: Young's modulus, anisotropy, texture, ideal orientation, α-iron, pole figure.

Методом Фурье-анализа изучена анизотропия модуля Юнга (*E*) в кристаллографических плоскостях основных идеальных ориентировок (ИО) текстур листов α-железа. Получены зависимости *E* от направления измерения, коэффициенты анизотропии и средние значения *E* в различных ИО текстур отжига и прокатки α-железа. Исследована текстура листов низкоуглеродистой стали DC04 (0.06 % C, до 0.35 % Mn, до 0.40 % Si, ~ 0.025 % S и P) после отжига и холодной прокатки. Набор ИО отожженных листов обеспечивает анизотропию *E* с максимумом в ПН и минимумом в НП + 45°. Прокатка формирует ИО, увеличивающие модуль Юнга в ПН и НП + 45°. Экспериментальные значения *E* находятся в удовлетворительном соответствии с результатами расчета из данных анизотропии ИО, полученных из рентгеновского текстурного эксперимента.

Аналіз анізотропії модуля Юнга ідеальної орієнтації α-залізних текстур. *Н.А.Волчок, Д.А.Дячок, З.А.Брюханова, Є.В.Дишлов.*

Методом Фур'є-аналізу вивчено анізотропію модуля Юнга (*E*) у кристалографічних площинах основних ідеальних орієнтувань (ІО) текстур листів α-заліза. Отримано залежності *E* від напрямку вимірювання, коефіцієнти анізотропії та середні значення *E* у різних ІО текстур відпалу і прокатки α-заліза. Досліджено текстуру листів низьковуглецевої сталі DC04 (0.06 % C, до 0.35 % Mn, до 0.40 % Si, ~ 0.025 % S і P) після відпалу і холодної прокатки. Набір ІО відпалених листів забезпечує анізотропію *E* з максимумом в ПН і мінімумом в НП + 45°. Прокатка формує ІО, що збільшують модуль Юнга в ПН і НП + 45°. Експериментальні значення *E* знаходяться у задовільній відповідності з результатами розрахунку із даних анізотропії ІО, отриманих з рентгенівського текстурного експерименту.

1. Introduction

The anisotropy of the elasticity of crystals in the approximation of the mechanics of continuous media is analytically described by means of fourth-rank tensors [1]. The elastic properties of single crystals are completely specified by a set of elastic constants. The number of independent constants depends on the symmetry of the crystal. For cubic crystals, there are three constants, for hexagonal — five, for trigonal — six, etc. Flat textures (sheet polycrystals textures) most often are described using ideal orientations (IO), which are characterized by a crystallographic plane (hkl) that coincides with the coordinate plane of the sample (for sheet polycrystals it is a rolling plane) and the crystallographic direction [*uvw*] which is coinciding with one of coordinates of the sample, for example, with the direction of rolling (RD).

Naturally, each of the IO has its own characteristic anisotropy of properties. In addition, the average property values for all directions in the crystal plane, which sets this IO, will also differ for different IO.

Usually, several IO are present in the texture, and the total anisotropy of the polycrystal is determined by the total contribution of the entire spectrum of IOs, taking into account their relative volume content in the texture. Therefore, the description of the anisotropy of properties in an arbitrary plane of a cubic crystal is of considerable interest for predicting the anisotropy of the properties of textured sheet polycrystals, as well as for considering issues related to the development and change of the texture during plastic deformation, heat treatment, and phase transformations.

Plastic deformation of elastoviscous metals and alloys leads to the formation of a scattered field of damage. This, in turn, is expressed in a decrease in the elastic moduli (modulus defect) with respect to the intact standard [2, 3]. Therefore, to separate the "texture" factor from the "defective" one in a deformed (damaged) polycrystal, the assessment of the contribution of various IOs to the total anisotropy of the elasticity of the polycrystal is essential.

In this work, we investigated the anisotropy of the Young's modulus and its average values for the main ideal orientations of the annealing and sliding textures of low carbon steel sheets.

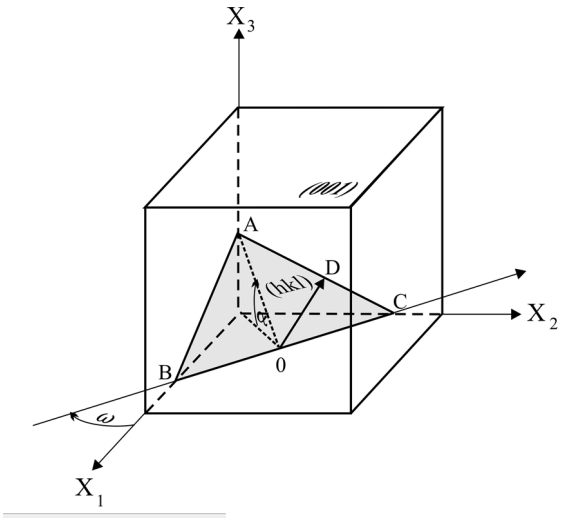

Fig. 1. Setting the position of the (hkl) plane by angles ω and α in a cubic crystal. BC is a zone of [$\bar{k}h0$] planes.

2. Anisotropy of elasticity of crystallographic planes of the cubic crystal

Cubic crystals are isotropic with respect to the physical properties of the second order tensor, but have anisotropy with respect to properties of a higher order tensor. In [4, 5], the position of the crystallographic plane (hkl) was defined by two angles ω and α; the first of these is equal to the angle between the axis of the plane zone [$\bar{k}h0$], which is given by BC line of intersection of the (hkl) plane with the coordinate (001) plane, and the [$\bar{1}00$] axis. The second angle is equal to the angle of inclination of the (hkl) plane to the (001) plane (Fig. 1).

Let us choose an arbitrary direction OA in the (hkl) plane. The equation for anisotropy of the Young's modulus in a cubic crystal [1] is expressed as

$$\frac{1}{E} = s_{11} - 2K\psi, \tag{1}$$

where s_{ij} are the single crystal compliance constants,

$$K = (s_{11} - s_{12} - \frac{1}{2}s_{44}), \tag{2}$$

$$\psi = a_1^2 a_2^2 + a_2^2 a_3^2 + a_1^2 a_3^2, \tag{3}$$

α_{ij} are direction cosines of the OD measurement direction. The expression for ψ is found for the OA direction. Using the methods of spherical trigonometry [6] for the

Table 1. The amplitudes of the harmonics of the Fourier series of the anisotropy functions of the crystallographic planes of some ideal orientations of a cubic crystal

Ideal orientations		The amplitudes of the harmonics of the Fourier series				
(hkl)	[$\bar{k}h0$]	A_0	A_2	A_4	B_2	B_4
100	010	0.21875	0.125	−0.09375	0	0
011	$\bar{1}$00	0.242188	−0.03125	0.011719	0	0
111	$\bar{1}$10	0.25	0	0	0	0
112	$\bar{1}$10	0.21875	−0.04167	0.048611	0	0
115	110	0.151235	−0.01646	0.107725	0	0
121	$\bar{2}$10	0.242188	0.052083	−0.05946	0.204124	0.142887
124	$\bar{2}$10	0.198342	−0.03827	0.070082	0.124696	0.461375
320	−230	0.21875	0.125	−0.09375	0	0
135	$\bar{3}$10	0.209184	−0.04082	0.059311	0.289767	0.869302
146	$\bar{4}$10	0.216347	−0.04161	0.051431	0.466508	1.221152
236	$\bar{3}$20	0.204693	−0.03993	0.063919	0.262391	0.857816
335	$\bar{3}$30	0.232693	−0.03894	0.029628	0	0
5$\bar{5}$4	550	0.247676	0.025826	-0.045567	0	0
358	530	0.221249	-0.0416	0.045567	0.983537	2.357427
$\bar{8}$ 6 2	$\bar{6}$ $\bar{8}$ 0	0.225545	0.106324	−0.08591	1.267212	0.684294
11 $\bar{8}$ 7	8 11 0	0.24568	0.036743	−0.05053	4.90458	3.751341

direction cosines of the OD direction, we obtain:

$$a_1 = \cos\omega\cos\varphi + \sin\omega\sin\varphi\cos\alpha, \quad (4)$$

$$a_2 = \cos\omega\sin\varphi\cos\alpha - \sin\omega\cos\varphi, \quad (5)$$

$$a_3 = \sin\alpha\sin\varphi. \quad (6)$$

After substitution, the expression (3) is reduced to the form corresponding to the Fourier series:

$$\psi = A_0 + A_2\cos2\varphi + A_4\cos4\varphi + B_2\sin2\varphi + B_4\sin4\varphi, \quad (7)$$

where A_i and B_i are the amplitudes of the harmonics of the Fourier series:

$$A_0 = \frac{1}{64}(8 - 24\sin^2\alpha - 21\sin^4\alpha - 3\sin^4\alpha\cos4\omega), \quad (8)$$

$$A_2 = -\frac{1}{16}[(6\sin^2\alpha - 7\sin^4\alpha) + (2\sin^2\alpha - \sin^4\alpha)\cos4\omega], \quad (9)$$

$$A_4 = -\frac{1}{64}[7\sin^2\alpha + (8\cos^2\alpha + \sin^4\alpha)\cos4\omega], \quad (10)$$

$$B_2 = -\frac{1}{8}\sin^2\alpha\cos\alpha\sin4\omega, \quad (11)$$

$$B_4 = -\frac{1}{16}\cos\alpha(1 + \cos^2\alpha)\sin4\omega. \quad (12)$$

Next we express the trigonometric values in formulas (7) to (12) in terms of Miller indices:

$$\cos\omega = \frac{k}{\sqrt{h^2 + k^2}}.$$

Then

$$\cos4\omega = 1 - 8\frac{h^2k^2}{(h^2 + k^2)^2}, \quad (13)$$

$$\sin4\omega = 4\frac{hk}{(h^2 + k^2)^2}(h^2 - k^2). \quad (14)$$

The angle α is equal to the angle of inclination of the plane to the plane (001).

Then

$$\cos\alpha = \frac{l}{\sqrt{h^2 + k^2 + l^2}}$$

and

$$\cos^2\alpha = \frac{l^2}{h^2 + k^2 + l^2}, \quad (15)$$

Table 2. The values of Young's modulus in different directions of crystallographic planes of ideal orientations {hkl} <$\bar{k}h0$> α-iron

Angle with [$\bar{k}h0$], degree	Young's modulus, GPa									
	Crystallographic plane of ideal orientation (hkl) [$\bar{k}h0$]									
	(100)	(011)	(111)	(112)	(122)	(124)	(135)	(146)	(236)	(358)
0	222.71	207.60	222.72	209.17	207.77	211.53	210.22	209.42	210.75	208.92
15	242.13	206.74	222.72	199.82	209.48	196.66	198.18	199.37	197.51	200.32
30	281.22	206.59	222.72	185.07	214.24	173.76	179.32	183.54	176.912	186.75
45	267.29	211.69	222.72	183.64	220.89	168.17	175.81	181.55	172.51	185.90
60	198.13	223.85	222.72	203.80	227.74	188.68	196.44	201.91	193.16	205.80
75	148.91	238.65	222.72	241.36	232.87	232.85	237.95	240.63	235.95	242.01
90	133.69	245.73	222.72	264.27	234.78	262.33	264.51	264.57	263.86	263.76
105	148.72	238.73	222.72	241.60	232.89	233.14	238.21	240.88	236.23	242.23
120	197.73	223.94	222.72	203.99	227.78	188.89	196.65	202.10	193.36	205.99
135	266.95	211.74	222.72	183.69	220.94	168.21	175.86	181.61	172.56	185.95
150	281.38	206.60	222.72	185.01	214.27	173.65	179.24	183.47	176.83	186.69
165	242.36	206.73	222.72	199.73	209.50	196.51	198.05	199.27	197.38	200.23
180	222,72	207.60	222.72	209.17	207.77	211.53	210.22	209.42	210.75	208.92
Average module, GPa	219.53	218.17	222.72	208.49	220.07	200.46	204.67	207.52	202.91	209.5
Coefficient anisotropy, η	0.525	0.159	0	0.305	0.115	0.358	0.335	0.314	0.346	0.295

$$\sin^2\alpha = \frac{h^2 + k^2}{h^2 + k^2 + l^2}. \qquad (16)$$

Table 1 shows the amplitudes of the harmonics of the anisotropy function ψ(φ) in the form of Fourier series for the crystallographic planes of some ideal orientations of a cubic crystal. The angle φ is measured from the axis [$\bar{k}h0$] of the zone (in Fig. 1, this is a vector $\overrightarrow{BC}$).

As can be seen from the Table, the main contribution to the elastic modulus anisotropy is made by the even harmonics of the Fourier series for the main IO with small indices. If the direction of the IO does not coincide with the direction of symmetry of the property, then odd harmonics appear. This is typical for IO with relatively high indices.

3. *Anisotropy of the Young's modulus of the main ideal orientations of α-iron sheet textures*

According to Table 1, the anisotropy of the Young's modulus of possible texture ideal orientations of low carbon steel sheets

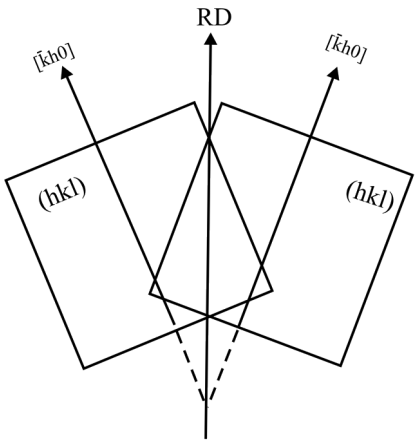

Fig. 2. About the symmetry of the (hkl) type orientations of [$\bar{k}h0$] relative to RD of sheets of cubic polycrystal.

was calculated. The constants of compliance in (1), (2), were used from [9]. The calculation results are shown in Table 2.

From Table 2 it follows that each of the ideal orientations has a certain anisotropy of the Young's modulus; the anisotropy is characterized by its average value and anisotropy coefficient

Table 3. The angles between the directions of the {hkl} <$\bar{k}h0$> orientations and the ideal texture orientations of the α-iron sheets

Ideal crystal orientation		Ideal orientation of texture		The angle between the directions of ideal orientations, degree
(hkl)	[$\bar{k}h0$]	(hkl)	[UVW]	
335	[$\bar{3}30$]	(335)	[71$\bar{2}$3]	120
112	[$\bar{1}10$]	(112)	[110]	90
320	[$\bar{2}30$]	(320)	[001]	90
100	[010]	(100)	[$\bar{3}10$]	71.6
001	[010]	(001)	[110]	45
112	[$\bar{1}10$]	(112)	[110]	90
111	[$\bar{1}10$]	(111)	[110]	90
111	[$\bar{1}10$]	(111)	[112]	90
115	[$\bar{1}10$]	(115)	[110]	90
115	[$\bar{1}10$]	(115)	[$\bar{5}52$]	90
221	[$\bar{2}20$]	(221)	[114]	90
221	[$\bar{2}20$]	(221)	[110]	90

$$\eta = \frac{E_{max} - E_{min}}{E_{max}}.$$

The (100) [*010*] orientation is characterized by the maximum E value in the (100) plane in the [*010*] + 45° direction. For (112), (124), (135), (146), (236), and (358) orientations, the Young's modulus takes the minimum value in the [$\bar{k}h0$] direction. The maximum Young's modulus for these orientations is in the direction of +90°.

The average E takes the maximum value for the IOs with crystallographic planes {111} (Table 2). For the IOs with planes from {110} to {124}, the average E values monotonously decrease to a cubic orientation of the {100} <$\bar{k}h0$> type, while the average value of the Young's modulus increases sharply. The behavior of the anisotropy coefficient E is the opposite (Table 2). When moving from orientations with the {100} plane to orientations with the {111} plane, the anisotropy coefficient E monotonously decreases from 0.525 to 0.295.

Typical ideal orientations for annealing textures of α-iron sheets are following: (335) [7 1$\bar{2}$ 3], (112) [110], (320) [001], and (100) [011]. The slip textures are characterized by: (001) [110], (112) [110], (111) [110], (111) [112], and (115) [110]. In the α-iron rolling textures, the presence of orientations formed due to twinning is also possible: (115) [552], (221) [114], (221) [110] [8, 9]. For these orientations, using the formula

$$\cos\varphi = \frac{U_1U_2 + V_1V_2 + W_1W_2}{\sqrt{U_1^2 + V_1^2 + W_1^2} \cdot \sqrt{U_2^2 + V_2^2 + W_2^2}} \quad [10],$$

we calculated the angles φ between the directions corresponding to the IOs and the directions [$\bar{k}h0$] (Table 3).

Next, we calculated the anisotropy of the Young's modulus for iron sheets' texture ideal orientations which directions do not coincide with the corresponding [$\bar{k}h0$] in Table 2. For the orientation directions forming the angles not equal to 0 and 90°, the anisotropy values were calculated taking into account symmetry with respect to the rolling direction (RD).

The results of the calculation of the E anisotropy in the plane of the iron sheets with texture ideal orientations after annealing, sliding and twinning are given in Table 4.

In addition to the set of ideal orientations present in the texture, the real anisotropy of a sheet polycrystal is determined by the scattering of the orientations. Naturally, the scattering reduces the anisotropy of each of the ideal orientations, since the resulting contribution of the diffuse orientation consists of the orientation itself and the similarly others but with different initial phases within the region of scattering.

The simultaneous action of several different orientations weakens their total action if their harmonics of the Fourier series are in antiphases. For example, orientations (335) [7 1$\bar{2}$ 3] and (112) [$\bar{1}$10],

Table 4. Anisotropy of the Young's modulus for ideal orientations of annealing and rolling textures of the α-iron sheets

Angle with RD, degree	Young's modulus, GPa						
	Crystallographic plane and direction of ideal orientation (hkl) [*uvw*]						
	(335) [71$\bar{2}$3]	(112) [$\bar{1}$10]	(320) [001]	(100) [$\bar{3}$10]	(001) [110]	(115) [110]	(221) [114]
0	250.4775	209.17	133,69	173.52	252.7592	238.8925	156.4689
15	229.2081	199.82	148.7194	200.49	231.7485	206.0911	170.8992
30	206.7087	185.07	197.7261	214.97	190.316	160.9817	213.7061
45	196.87	183.64	266.9454	219.93	171.518	143.696	262.5205
60	199.4446	203.8	281.3797	244.83	196.4057	155.7798	264.0763
75	205.5486	241.36	242.3552	252.05	242.3859	192.1688	231.9981
90	207.971	264.27	222.7179	242.36	265.1852	218.3549	216.4883
105	205.5486	241.6	222.7171	252.05	242.637	192.4204	216.4877
120	199.4446	203.99	242.1317	244.83	196.6642	155.9391	231.8218
135	196.87	183.69	281.2173	219.93	171.5382	143.6828	263.9207
150	206.7087	185.01	267.286	214.97	190.0923	160.7835	262.7157
165	229.2081	199.73	198.1301	200.49	231.5169	205.7765	214.0322
180	250.4775	209.17	148.909	173.52	274.255	238.8925	171.0773
Average module, GPa	214.1912	208.4862	219.5327	219.5338	219.5338	185.6507	221.2471
Coefficient anisotropy, η	21.40211	30.51046	52.4877	31.15652	32.02215	39.85462	40.7486

being simultaneously present in the texture, reduce the anisotropy of elastic properties. Thus, it is possible to achieve isotropy of sheets not only by weakening the texture itself due to increasing the scattering of the main orientations, but also by developing IOs with opposite phases of the harmonics in the corresponding Fourier series.

4. Results and discussion

We studied the texture of DC04 steel sheets (0.06 % C, up to 0.35 % Mn, up to 0.40 % Si, ~ 0.025 % S and P) of 2 mm thickness after recrystallization annealing and straight symmetric rolling up to 50 % deformation according to the thickness. Disc-shaped samples were cut out of the sheets for X-ray studies of the texture, and rectangular samples 10×80 mm^2 in size for measuring the Young's modulus by the dynamic method according to the natural frequency [11]. The rectangular samples were cut out from the sheets at different angles to the RN after every 15°. The frequency was determined using the Spectra PLUS computer program [12]. The texture was studied by the X-ray diffraction method with the construction of straight pole figures (PF) using the Schulz method "on reflection" [8] on a modernized diffractometer DRON-3M in Cu–Kα radiation. PFs of {110}, {200}, and {210} were built in the levels of average pole density. The defocusing that occurs when the sample is tilted to the goniometer axis was taken into account with the aid of a powder reference.

Fig. 3 shows PFs of {110}, {200} for DC04 steel sheets in the state after recrystallization annealing and cold rolling to 50 reduction.

The central part of the {200} PF for the original steel sheets is filled with the outputs of the normals with the greatest intensity. This corresponds to the presence of the {100} <011> orientation in the texture of the sheets. The pole density maxima on the large circle in the RD + 45° correspond to the same orientation. The {100} <011> is one of the typical orientations of the rolling texture in bcc metals.

Another typical orientation for textures of bcc metals sheets is {112} <110>. The increased pole density is observed at an angular distance of 35° from the center. At the {200} PF, the areas of increased pole density are also distinguished at the angular distance of 60° from the center to

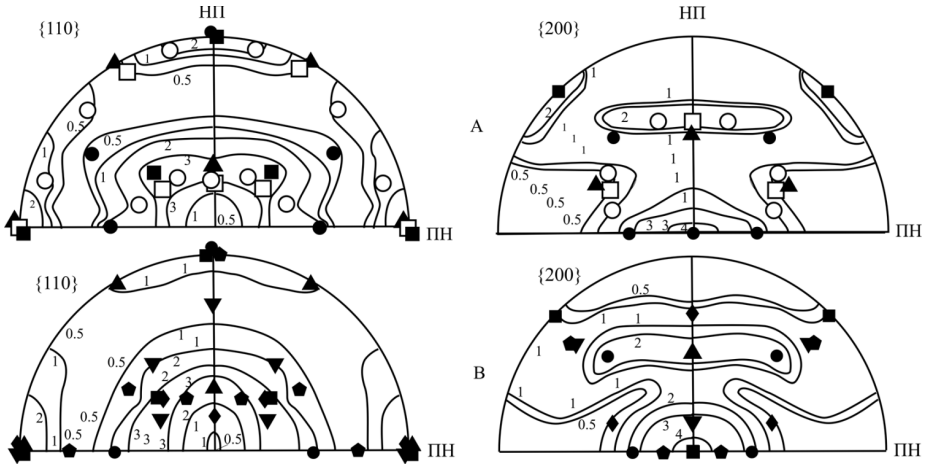

Fig. 3. Pole {110} and {200} figures for sheets of steel DC04 A — annealed, B — after cold rolling; and the ideal orientations corresponding to texture: • (112) [110]; ■ — (001) [110]; ▲ — (111) [112]; ▼ (115) [552]; ♦ — (221) [114]; ✸ — (115) [110]; O — (11 8 7) [135]; □ — (554) [225].

the RD and on RD±40° along the arc of the large circle. These areas correspond to orientations with high indices close to {111} <112>:{11 8 7} <135> and {554} <225>. The {111} <112> orientation is one of the texture orientations of rolled bcc metals. At the PF, it goes beyond the regions with high pole density, that means, it enters the scattering region of the orientations {1187} <135> and {554} <225>.

At the {110} PF, the areas of increased pole density are concentrated around the center of the PF at a distance of 30–70° from it, as well as in the large circle — in RD, RD±30°, in transverse direction (TD) and TD±50°. These areas are well filed by the outputs of the normals to the ideal orientations found by analyzing the {200} PFs, including the orientation {111} <112>. The {211} PFs are consistent with {200} and {110} PFs. Here, they are not given due to the congestion with symbols of ideal orientations.

In general, the texture of the original steel sheets (delivery status) can be characterized by rolling texture typical orientations of the bcc metals: {112} <110>, {100} <011>, orientations close to {111} <112>:{11 8 7} <135>, and {554} <225>. The {111} <112> orientation characteristic to rolling textures of bcc metals, can also be considered as one of the solutions for the description of the texture of the original sheets. At the {110} and {112} PFs, this orientation is in the region of increased pole density, and at the {200} PF, it enters the orientation scattering area of {11 8 7} <135> and {554} <225>. Orientations with high indices are attributed to the components of annealing textures [11] of bcc metals. A theoretical analysis of the orientations of recrystallized grains, which are capable to grow in multi-component deformation textures, showed that the strain {112} <110>, {100} <011>, {111} <112> orientations can develop to the {11 8 7} <135> and {554} <225> orientation types.

In contrast to the {200} PF of the original sheet, the region of maximum pole density on the PF from rolled steel sheets is shifted from the position at a distance of 55–70° to the position specified by the angles 50–60° from the center of the PF. It corresponds to the transition from orientations with high indices to the {111} <112> orientation. The outputs of the normals to the {112} <110> orientation fall into this area. The {110} PF is consistent with {200} PF. In addition to the indicated orientations, the areas of increased pole density of this PF include the {221} <114> orientation. At the {200} PF, this orientation is present in the scattering region. On the {112} PF, the areas of maximum pole density are located in the center of the PF and around the center and extended by 40° in RD and 50° in TD. This area includes all texture description solutions found from {200} and {110}.

Thus, as a result of direct rolling, a typical rolling texture of bcc metals is formed in steel sheets with the {001} <110>, {112} <110>, and {111} <112> orientations and {115} <552>, {115} <110>, and {221} <114> orientations close to the rolling texture orientation. The crystallographic (111) plane is

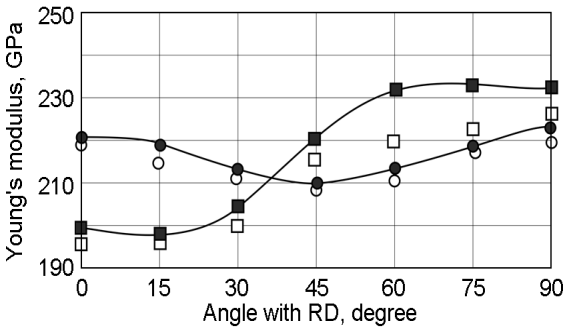

Fig. 4. Anisotropy of the Young's modulus for DC04 steel sheets after • — annealing and ■ — rolling deformation. O , □ — experimental values of the Young's modulus for annealed and deformed sheets of DC04 steel.

isotropic in terms of elastic properties (Table 2), but has a high average Young's modulus. For bcc iron, it is 222 GPa. The planes close to it, for example, {11 8 7} <135> and {554} <225>, are also weakly anisotropic. The main contribution to the anisotropy of the elastic properties of the original sheets is made by the highly anisotropic orientations {112} <110> and {100} <011>. The E anisotropy of these two orientations gives curves with a maximum in the TD and a minimum in RD + 45° (Fig. 4). The average modulus for these two orientations is 219 GPa. The isotropic orientations of the {111} type can somewhat increase the mean modulus, but they do not change the nature of anisotropy. The experimental points shown in the figure repeat the nature of the calculated E anisotropy, but lie somewhat lower than the theoretical ones. Such a deviation is due, firstly, to the approximation of the selected single crystal compliance constants, which were values for pure iron, and, secondly, to the real steel defect structure lowering the Young's modulus values in all directions in the sheet [11].

After rolling, the {115} <552>, {115} <110> and {221} <114> IOs are superimposed on the already existing texture with orientations of deformation and annealing. The first two increase the value of the Young's modulus in the TD, and the last IO increases E in the RD + 45°. The experimental values of E correspond to the nature of the calculated elastic anisotropy.

In general, taking into account the made approximations, the fit of the experimental data for elastic anisotropy E and calculated from observed IOs in the PFs for annealed and deformed low carbon steel sheets is satisfactory.

5. Conclusions

Ideal orientations of flat textures in cubic metals give their own characteristic anisotropy of elastic properties, which is determined by the crystallographic plane, the direction of reference of the measurement angle, and single crystal characteristics of elasticity. The average values of Young's modulus for various IOs of iron textures vary within 20 %. The presence of various IOs in the texture affects the anisotropy of the elastic properties and their final values. The texture of low carbon steel sheets DC04 (0.06 % C, up to 0.35 % Mn, up to 0.40 % Si, ~ 0.025 % S and P) after recrystallization annealing is characterized by the orientations: {112} <110> and {100} <011>, and the orientations close to {111} <112>: {11 8 7} 3, and {554} <225>. As a result of direct rolling, a typical rolling texture of bcc metals is formed in the steel sheets with the {001} <110>, {112} <110>, and {111} <112> orientations, and {115} <552>, {115} <110>, and {221} <114> orientations close to the rolling texture orientation. The main contribution to the anisotropy of the elastic properties of the annealed sheets is made by the highly anisotropic orientations {112} <110>, and {100} <011>. Their total anisotropy E is characterized by a maximum in the transverse direction and a minimum in the RD + 45°. The development of the {115} <552>, {115} <110> and {221} <114> IOs as a result of cold rolling, increases the value of the Young's modulus in the TD and RD + 45°. Direct measurements of the Young's modulus for the undeformed and rolled sheets of low carbon steel are in satisfactory agreement with the results of the calculation of the E anisotropy from the IO anisotropy data obtained from the X-ray texture experiment.

References

1. J.F.Nye, Physical Properties of Crystals, Claremont Press, Oxford (1964).
2. J.A.Lemaitre, Course on Damage Mechanics, Springer-Verlag, Berlin (1992).
3. L.N.Larikov, Healing Defects, Naukova Dumka, Kyiv (1980).
4. A.Ye.Briukhanov, *Techn. Phys. J.*, **7**, 2065 (1937).
5. A.A.Bryukhanov, *Izv. Vyssh. Uchebn. Zaved., Fiz.*, **4**, 153 (1977).
6. I.R.Shafarevich, A.O.Remizov, Linear Algebra and Geometry, State Publishing House of Physics-math. Lit., Moscow (2009) [in Russian].

7. G.Schulze, Metallphysik, Akademie-Verlag, Berlin (1967).
8. G.Wassermann, J.Grewen, Texturen Metallischer Werkstoffe, Springer, Berlin (1962).
9. Ya.D.Vishnyakov, A.A.Babareko, S.A.Vladimirov, I.V.Egiz, Theory of Formation of Textures in Metals and Alloys, Nauka, Moscow (1979) [in Russian].
10. L.I.Mirkin, Handbook of X-ray Analysis of Polycrystals, State Publishing House of Physics-math Lit., Moscow (1961) [in Russian].
11. G.Gerstein, A.Briukhanov, F.Gutknecht, N.Volchok, Proc. 17th Intern. Conf. on Metal Forming, METAL FORMING 2018 September 16–19, 2018, Loisir Hotel Toyohashi, Toyohashi, Japan, Elsevier, Procedia Manufacturing, Special Issues, v.1 (2018), p.527.
12. Spectra PLUS 5.0.23 (FFT Spectral Analysis System).